Pushing Wi-Fi HaLow to the Extreme Edge: A Performance Study on a Low-Power IoT Node

Nicolas Schärer, Tommaso Polonelli, and Michele Magno
Department of Information Technology and Electrical Engineering, ETH Zurich, Zurich, Switzerland

2025 10th International Workshop on Advances in Sensors and Interfaces (IWASI) | 979-8-3315-6578-7/25/$31.00 ©2025 IEEE | DOI: 10.1109/IWASI66786.2025.11121933

***Abstract*—Wi-Fi HaLow (IEEE 802.11ah) is a novel emerging wireless standard designed for low-power, long-range data communication for Internet of Things (IoT) applications [1]. This paper presents a practical performance evaluation of Wi-Fi HaLow (IEEE 802.11ah) using off-the-shelf hardware, focusing on application-level energy efficiency and throughput across varying distances emulated via the free-space path loss (FSPL) model. Our experiments demonstrate energy per bit (EPB) as low as 27 nJ bit^{-1} (and 45 nJ bit^{-1} at an equivalent 158 m) and effective bit rates (EBR) from 0.15 Mbit s^{-1} to 18 Mbit s^{-1} over FSPL-calculated distances up to nearly 50 km. A key contribution is the quantitative analysis of HaLow's potential to enhance a wind turbine blade monitoring Wireless Sensor Network (WSN), projecting a two-fold EPB reduction and a tenfold EBR increase compared to BLE. These findings provide critical benchmarks for HaLow's practical deployment, underscoring its capacity to enable demanding IoT applications by uniquely balancing range, data rate, and power efficiency, thereby addressing limitations of existing wireless technologies.**

***Index Terms*—Low-Power, Long-Range, Telecommunication, IoT, Wi-Fi, HaLow, IEEE 802.11ah, Extreme Edge, WSN, FSPL**

I. Introduction

The proliferation of IoT devices necessitates wireless communication technologies that can deliver long-range connectivity, high data throughput, and low power consumption [2].

Wi-Fi HaLow is a novel and emerging sub-1 GHz WLAN standard designed for low-power, long-range IoT applications [3]. Operating in the 750 MHz to 928 MHz band, it offers better propagation and penetration than traditional 2.4 GHz/5 GHz Wi-Fi, supporting communication distances beyond 1 km in typical outdoor settings [4], [5]. HaLow enables up to 8191 devices per access point and supports scalable bandwidths (1 MHz to 16 MHz) and modulation schemes from BPSK to 256-QAM. Data rates range from 150 kbit s^{-1} to 86.7 Mbit s^{-1}, making it suitable for applications requiring both range and moderate throughput. It also aims to transparently fit into classical IP networks, easing the integration of nodes into larger IoT networks. Power-saving mechanisms such as Target Wake Time (TWT), Restricted Access Window (RAW), and optimized MAC headers aim to enable multi-year battery operation.

The purpose of this paper is to provide a rigorous, empirical evaluation of Wi-Fi HaLow's practical performance using readily deployable commercial hardware, addressing the need for concrete data to guide its adoption in diverse IoT scenarios, particularly for demanding WSN applications. While HaLow's specifications are promising, detailed characterization of its application-level performance in realistic or emulated long-range conditions remains an area requiring further investigation. This work aims to fill this gap. The main scientific contributions of this paper, advancing the practical understanding of Wi-Fi HaLow, are: *(i)* A reproducible HaLow testbed using commercial, edge-ready platforms to emulate real-world link conditions (via FSPL), crucial for assessing practical deployability. *(ii)* Rigorous application-level energy efficiency benchmarks (e.g., 27 nJ bit^{-1}), providing scarce data vital for designing long-lifetime battery-powered IoT nodes. *(iii)* Quantification of HaLow's long-range, high-throughput capabilities (EBR 0.375 Mbit s^{-1} to 17.9 Mbit s^{-1} over FSPL distances up to 49.9 km), vital for data-intensive, extended-reach applications. *(iv)* A novel case study demonstrating HaLow's potential to significantly enhance a wind turbine monitoring WSN (two-fold EPB reduction, tenfold EBR increase vs. BLE), enabling advanced edge applications. *(v)* An evidence-based comparison with key IoT protocols (BLE, ZigBee, UWB, Wi-Fi, LoRaWAN, NB-IoT, LTE-M), clearly delineating HaLow's unique value based on our experimental findings.

The experiments were performed within the MISTERY project funded by the French National Research Agency (ANR PRCI grant no. 266157) and the Swiss National Science Foundation (grant no. 200021L 21271).

II. Related Works

Wireless communication technologies form the backbone of IoT systems [6], offering various trade-offs between range, data rate, and power consumption. This section provides an overview of common and emerging IoT communication protocols, with a focus on Wi-Fi HaLow (IEEE 802.11ah), highlighting its performance through recent field evaluations.

Short-range technologies such as Bluetooth Low Energy (BLE), ZigBee, and Ultra-Wideband (UWB) are optimized for low power consumption [7] and operate in the 2.4 GHz or higher frequency bands. BLE offers low EPB [8] (1×10^{-7} J bit^{-1} to 1×10^{-6} J bit^{-1}) and supports modest throughput (1 Mbit s^{-1}) with limited range (50 m). ZigBee is ideal for mesh networking with a 250 kbit s^{-1} data rate [7]. UWB supports precise ranging and short high-speed bursts but with a limited communication range (10 m to 50 m) [9].

Wi-Fi(802.11b/g/n/ac) delivers high throughput (up to several Gbps) but at the cost of higher power consumption and moderate range. In contrast, Wi-Fi HaLow, operating in the

TABLE I
PERFORMANCE COMPARISON OF COMMON IOT WIRELESS PROTOCOLS FROM SOA [13], [14] AND THIS WORK.

Protocol	EBR (kbps)	EPB (J/bit)	Range
BLE	∼800	10^{-7}–10^{-6}	50–100 m
ZigBee	250	2×10^{-7}	10–100 m
UWB	110–6800	2×10^{-6}	10–50 m
Wi-Fi	10^{5}–10^{6}	10^{-8}–10^{-6}	100–300 m
LoRaWAN	0.3–5	10^{-3}–10^{-2}	1–20 km
NB-IoT	50–100	10^{-4}–10^{-3}	10–100 km
LTE-M	∼1000	10^{-5}–10^{-6}	5–10 km
Wi-Fi HaLow	150–18000	10^{-8}–10^{-6}	>1 km

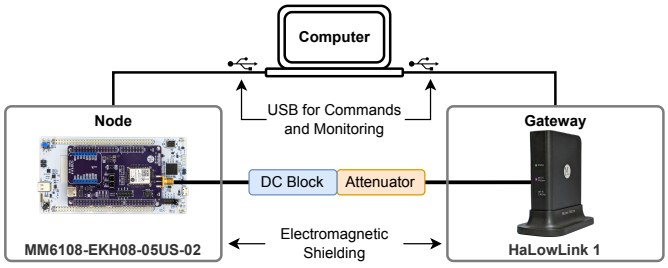

Fig. 1. Test setup description. The two devices are connected through SMA cables, attenuators, and a DC-block to perform conducted tests. The computer issues the test commands and is used to collect the results.

sub-1 GHz band, offers long-range connectivity (over 1 km) with improved wall penetration and moderate throughput (0.15 Mbit s^{-1} to 18 Mbit s^{-1}). Field tests demonstrate Wi-Fi HaLow's capacity to maintain multi-Mbps throughput at kilometer-scale distances, with comparable energy efficiency compared to other IoT communication standards [3]–[5].

Cellular IoT standards such as NB-IoT and LTE-M [10], [11] leverage existing infrastructure to provide reliable, long-range coverage. NB-IoT achieves up to 100 kbit s^{-1} with excellent indoor penetration and EPB in the mJ bit^{-1} range [11]. LTE-M offers higher throughput, up to 1 Mbit s^{-1}.

LoRa and LoRaWAN [12] use chirp spread-spectrum modulation for ultra-long-range communication at low data rates (0.3 kbit s^{-1} to 50 kbit s^{-1}). They are ideal for battery-operated sensors with minimal data needs, though EPB increases significantly at low spreading factors. Enhancements like Slotted LoRaWAN (S-LoRaWAN) and Enhanced LoRaWAN (E-LoRaWAN) aim to improve network scalability and QoS.

Table I summarizes the trade-offs between different protocols in terms of effective bitrate (EBR), EPB, and coverage. Selecting the optimal protocol remains a challenge, as IoT applications often demand conflicting features such as ultra-low power and long-range communication. A heterogeneous approach that leverages multiple technologies is often necessary to meet these diverse requirements.

In the case of continuous sensor data streaming for large structure monitoring, the communication can sometimes be the bottleneck of the system. An example is the monitoring of wind turbine blades [8]. In this scenario the distance to be covered is at least 100 m, excluding UWB from the options. The selected option in the Aerosense project [8] is BLE as it offers good coverage and decent throughput. However, the sensors generate more data (4.2 Mbit s^{-1}) than the maximum BLE throughput (1 Mbit s^{-1}), making continuous real-time monitoring impossible. The existing body of literature on Wi-Fi HaLow performance is largely divided between theoretical studies based on simulations [1], [15], [16] and experimental field tests using high-level computing platforms [3], [5], [17]–[19], both of which present challenges in terms of reproducibility and practical relevance for constrained IoT nodes. Lee et al. [4] developed a System-on-Chip (SoC) and show promising results in terms of coverage and power consumption. However, as this is custom hardware, it is not broadly available and limits its large-scale deployment on the field for IoT devices.

A critical limitation of current literature is the lack of reproducible, application-level evaluations of Wi-Fi HaLow on embedded systems, particularly regarding energy consumption per bit [20]. While energy models exist for certain technologies, experimental data on end-to-end energy efficiency at the application level is scarce, making it difficult to compare technologies in practical deployment contexts [21]. This lack of data also hinders comparisons with other low-power communication protocols such as LoRaWAN, BLE 5, UWB [9], and Wi-Fi 7, which are increasingly used in various IoT scenarios [14].

Moreover, field-based results are highly dependent on environmental conditions and test configurations, making comparisons between studies difficult [11]. Few works address reproducibility or provide modular, open test setups that can be easily adopted by other researchers or practitioners.

III. METHODOLOGY

To accurately evaluate the performance of Wi-Fi HaLow in the context of low-power wireless sensors and IoT applications, a point-to-point setup is proposed utilizing two devices from *Morse Micro*: the *MM6108-EKH08-05US-02* evaluation kit (evalkit) as the IoT node, and the *HaLowLink 1* as the gateway. They differentiate in their roles and form factors: the *MM6108-EKH08-05US-02* is a flexible evalkit for the IoT node, interfacing with a standard STM32 Nucleo development board from STMicroelectronics. The *HaLowLink 1* is an end-product acting as an access point for the HaLow network and allows for the integration of HaLow devices into IP networks over Ethernet or traditional Wi-Fi. This ecosystem is selected due to its state-of-the-art radio performance, the ease of integration offered through the provided tools, and the standard Nucleo board compatibility for the node, making it well-suited for evaluating HaLow in diverse IoT scenarios. Both devices are based on the *MM6108-MF08651-US* module, which is a fully integrated Wi-Fi HaLow solution built around the core MM6108 SoC. Using such a module enables an easy integration into custom designs as it incorporates essential RF components like a high linearity LNA, SAW filter, T/R switch, 32 MHz crystal oscillator, and necessary RF filters and matching circuitry, a Power Management Unit (PMU),

and provides digital interfaces for host communication. An external Front-End Module (FEM) is also embedded to achieve a maximum transmit power of up to 21 dBm, a significant increase compared to the 6 dBm limit of the bare SoC, extending the maximum range.

Tests are conducted using two distinct bandwidth configurations: 8 MHz and 1 MHz. This selection is made to characterize the performance under what represents near 'best-case' and 'worst-case' scenarios in terms of data throughput and coverage, respectively. The 8 MHz bandwidth offers the highest theoretical data rates supported by the standard, making it ideal for assessing maximum throughput performance under favorable link conditions. The 1 MHz bandwidth, while offering lower data rates, benefits from an improved link budget due to its narrower channel, allowing for testing the maximum achievable range and reliability under challenging signal attenuation. The performance characteristics for these intermediate configurations are expected to fall predictably between the extremes established by the 1 MHz and 8 MHz tests.

A. Test Setup

This section presents the test setup used to evaluate the throughput depending on the link quality, together with the energy needed for communication. The test setup designed to evaluate the performance of the novel WiFi Halow protocol in a controlled environment is described in Figure 1. It consists of a direct wired connection between the two devices, established using an SMA cable, a DC-Block to manage potential voltage differences, and variable attenuators. These attenuators introduce a controlled signal loss to simulate different link conditions, such as varying distances or propagation losses. To ensure that the RF signal transmission occurs only through this wired path (cable, DC-Block, attenuators) and not through indirect radiation between the devices, each device is electromagnetically isolated from the other. By systematically changing the value of the attenuator, repeatable performance data can be gathered under a range of simulated signal strengths.

The experimental evaluation quantifies the performance of the Wi-Fi HaLow link using the network testing tool *iperf*. A unidirectional UDP traffic stream is generated over a fixed duration of 10 seconds. In this point-to-point configuration, the IoT node is configured as the *iperf* client, transmitting data packets towards the gateway (HaLowLink 1), which functions as the *iperf* server. This simulates an edge device continuously transmitting sensor data. During each 10-second test interval, critical parameters are monitored and recorded. These include the instantaneous Modulation and Coding Scheme (MCS, described in Table II) selected by the physical layer, the applied signal attenuation, the power consumption drawn by the transmitting node, the achieved UDP payload throughput, and the percentage of lost UDP packets. Monitoring these parameters allows for the characterization of Wi-Fi HaLow in terms of data transfer, energy consumption, and reliability with a reproducible test setup. The key parameters are reported in Table IV

The RF output power for each device, the IoT node, and the gateway, is precisely measured before conducting the link performance tests. This is achieved by configuring each device to transmit a signal with a bandwidth of 1 MHz centered at a frequency of 919.5 MHz. The signal is then analyzed using a *Rohde & Schwarz FSIQ 3* signal analyzer operated in zero-span mode. This measurement technique allows for the accurate determination of the signal strength at the output port of each device during transmission. The measured output power for both the MM6108-EKH08-05US-02 node and the HaLowLink 1 gateway is 21 dBm, a result consistent with the maximum transmit power advertised by the manufacturer. The same process is employed to confirm the effective attenuation of the attenuators. The tests are conducted with the different attenuation values described in Table IV.

B. Distance Estimation

To convert the measured signal attenuation into an equivalent distance, the standard Free-Space Path Loss (FSPL) [22] model is inverted. Typically, FSPL predicts received power at a known distance by computing the expected path loss. Here, it is used to derive the transmitter–receiver distance from a conducted-mode measurement with attenuators of A_{att} (dB). In this context, PL_{dB} denotes only the free-space loss, excluding antenna gains, which are handled separately in the link budget. In eq. (1), we define P_r the received power (dBm) and P_t the transmitted power (dBm), while G_t, G_r are the transmitter and receiver antenna gains (dBi).

$$P_r = P_t + G_t + G_r - PL_{\mathrm{dB}} \tag{1}$$

To reflect the real-case scenario, two antennas of $G_t = G_r = 2.34$ (dBi) gain are chosen as it corresponds to the recommended antennas for the devices used in the test setup. In Equation (2), PL_{dB} is the path loss in free space (dB), d the distance between antennas in meters and, lastly, c the speed of light in vacuum ($\approx 3 \times 10^8$ m/s). The resulting distance d is reported in Equation (3).

$$PL_{\mathrm{dB}} = 20\log_{10}(d) + 20\log_{10}(f) + 20\log_{10}\left(\frac{4\pi}{c}\right) \tag{2}$$

$$d = 10^{\left(PL_{\mathrm{dB}} - 20\log_{10}(f) - 20\log_{10}\left(\frac{4\pi}{c}\right)\right)/20} \tag{3}$$

Both antenna gains are added in Equation (4). Lastly, substituting Equation (4) into Equation (3) yields the equivalent free-space distance in Equation (5).

$$PL_{\mathrm{dB}} = A_{\mathrm{att}} + G_t + G_r = A_{\mathrm{att}} + 4.68 \tag{4}$$

$$d = 10^{\left(A_{\mathrm{att}} + 4.68 - 20\log_{10}(f) - 20\log_{10}\left(\frac{4\pi}{c}\right)\right)/20} \tag{5}$$

It is important to note that the distance calculated using this method represents a theoretical value based on the ideal FSPL model. It does not account for real-world complexities such as multipath fading, reflections, absorption by objects,

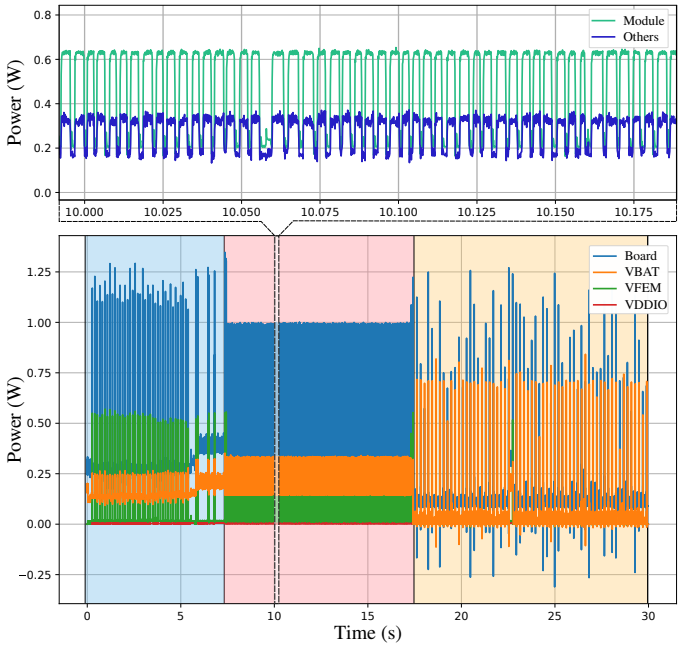

Fig. 2. Power consumption over time when conducting a performance test at 8 MHz with the RF output power set to 21 dBm. The bottom plot shows the full 30 seconds of acquisition with all the acquired traces. Three phases are observable, highlighted by three different background colors. A zoomed in view of the power consumption is shown on the top plot, and the measured traces are combined in either *Module* or *Others*.

interference in the operating band, antenna polarization mismatches, or the effects of device movement. This calculated distance serves primarily as a comparative metric to provide an intuitive sense of the signal loss in terms of distance under highly idealized conditions and to compare our results one-to-one with the literature.

IV. Results

A. Power Consumption

The power is measured for two separate output power, 21 dBm and 0 dBm, and two different bandwidths, 8 MHz and 1 MHz. They are measured for different MCS, but the impact of the modulation is negligible on power consumption. The results of the measurement are presented in Table III. The power consumption is measured during 30 seconds using a *Keysight N6705C* power analyzer while performing a performance test. The module requires power for the FEM, the VBAT and VDDIO pins of the MM6108. The current going to those pins is measured and summed up to infer the module's power consumption. The power consumption of the whole evalkit is also measured. The power consumption of the module is retrieved from the one of the whole board to provide the *Others* power consumption, which includes the microcontroller as well as the conversion losses and the board LEDs. An example of such an acquisition is shown in Figure 2. Three phases are observable on the bottom plot. The first shows the connection phase, where the node tries to connect to the gateway. Then, the performance test is initiated and lasts approximately ten seconds. The impact of each single packet transfer is observable in the top plot. Then, the node goes to a lower-power mode where it still regularly exchanges beacons to the gateway and listens for incoming messages. In this state, the node is still reachable from the gateway and the network. When in the listen phase, the module consumes 2.7 mW on average for the 8 MHz bandwidth, and 3.8 mW for the 1 MHz one. The maximum instantaneous power consumption of the whole system is 1.25 W,. The rest of the electronics consumes between 200 mW and 350 mW when transmitting. This is mostly due to the microcontroller, and optimizations are possible to bring this power down. While transmitting, VBAT, which powers the core of the HaLow SoC, and VFEM, which provides the current to the FEM, consume the most power. VDDIO is negligible in comparison.

B. Coverage

Detailed performance test results are provided in Table IV. The metrics reported include the applied attenuation, *Att*, the PHY throughput, *PHY*, directly obtained from the Modulation and Coding Scheme used, the UDP payload throughput, determined via iperf testing, *UDP*, and the resulting UDP packet loss, *PL*. The table also shows the distance, *d*, calculated from the attenuation based on the method detailed in Section III, and the energy consumed per bit, *EPB*, computed by dividing the UDP throughput by the corresponding average power consumption at 21 dBm output power. The maximum achieved throughput is 17.9 Mbit s^{-1} with a low UDP packet loss of 1.5 %. Although the equivalent distance for this optimal performance is only 46 cm, making it irrelevant for real use, it serves as a useful benchmark. This point also demonstrates good energy efficiency, with an energy consumption per bit of just 27 nJ bit^{-1}. At a distance of 159 m, the system maintains a high throughput of 10.7 Mbit s^{-1} with minimal UDP packet loss at 2.2 %. Up to this range, the highest throughput MCS is used, corresponding to a PHY throughput of 32.5 Mbit s^{-1}. Beyond this distance, for an equivalent free-space path loss corresponding to 4991 m, the PHY throughput decreases to 29.5 Mbit s^{-1}. This reduction is consistent with the expected MCS downgrade due to reduced received power, as summarized in Table II. Specifically, the received power is given by

$$P_r = P_t - PL_{\mathrm{dB}} \tag{6}$$

with $P_t = 21\,\mathrm{dBm}$, $PL_{\mathrm{dB}} = 101\,\mathrm{dB}$, and thus $P_r = -80\,\mathrm{dBm}$, which falls below the sensitivity threshold for MCS index 0 ($-77\,\mathrm{dBm}$). Another drop happens in both UDP (1.21 Mbit s^{-1}) and PHY (9.7 Mbit s^{-1}) throughput when nearing the sensitivity floor of the module for the 8 MHz bandwidth (–97 dBm). For the 1 MHz bandwidth, in the best case scenario, the throughput reaches 2.46 Mbit s^{-1} and remains above 1 Mbit s^{-1} for an attenuation of 101 dB. The maximum attenuation at which a communication happens is 121 dB, but the throughput is drastically reduced (375 kbit s^{-1}).

When using an attenuation of 121 dB for 8 MHz and 131 dB for 1 MHz, the connection cannot be established. The module output power is set at 21 dBm, therefore, the module's

TABLE II
ADVERTISED MODULE PERFORMANCE CHARACTERISTICS (MM6108)

MCS Index	Modulation Scheme	Coding Rate	PHY Rate (kbps) per BW				Minimum Receive sensitivity (dBm) per BW			
			1 MHz	2 MHz	4 MHz	8 MHz	1 MHz	2 MHz	4 MHz	8 MHz
0	BPSK	1/2	333	722	1500	3250	-105	-103	-101	-97
1	QPSK	1/2	667	1444	3000	6500	-102	-100	-97	-93
2	QPSK	3/4	1000	2167	4500	9750	-99	-97	-95	-91
3	16-QAM	1/2	1333	2889	6000	13000	-96	-94	-91	-88
4	16-QAM	3/4	2000	4333	9000	19500	-93	-90	-88	-85
5	64-QAM	2/3	2667	5778	12000	26000	-89	-87	-84	-80
6	64-QAM	3/4	3000	6500	13500	29250	-88	-85	-83	-79
7	64-QAM	5/6	3333	7222	15000	32500	-87	-84	-81	-77

TABLE III
POWER CONSUMPTION WHILE PERFORMING THE PERFORMANCE TEST

Output Power (dBm)	Bandwidth (MHz)	Average Power (mW)
21	8	486
21	1	492
0	8	380
0	1	318

TABLE IV
PERFORMANCE TEST RESULTS BY BANDWIDTH AND ATTENUATION

Att (dB)	PHY (Mbps)	UDP (Mbps)	PL (%)	d (m)	EPB (nJ)
8 MHz					
20	32.5	17.9	1.5	0.46	27
41	32.5	11.4	2.2	5	43
71	32.5	10.7	2.2	158	45
101	29.2	7.44	8.6	4991	65
114	9.7	1.21	22	22295	399
1 MHz					
20	3.4	2.46	16	0.46	200
41	3	1.24	16	5	395
101	2	1.31	19	4991	376
114	2.7	0.848	37	22295	580
121	2	0.375	62	49912	1312

sensitivity is between −93 dBm and −100 dBm for 8 MHz and between 100 dBm and −110 dBm for 1 MHz. This aligns with the module's expected characteristics, as described in Table II, with a best sensitivity (MCS = 0) of −97 dBm and −105 dBm for a bandwidth of 8 MHz and 1 MHz respectively. These results confirm the absence of RF leakage and that our test methodology is consistent. In general, the results also align with the other different sensitivities described by the manufacturer and shown in Table II.

From these tests, the 8 MHz bandwidth seems generally superior to the 1 MHz one, except when the link quality does not allow to use it. However, in challenging real-world environments, a narrower 1 MHz bandwidth provides a more robust link by concentrating signal energy and spanning less spectrum, which improves the signal-to-noise ratio and reduces vulnerability to interference compared to a wider 8 MHz band. The flexibility allowed by the different usable bandwidths is a great asset of this technology and can be used to optimally adapt to the RF environment.

From our tests, HaLow could theoretically cover distances of around 50 km. However, the literature shows test fields reliably working only up to around 1 km. This is probably due to the limitations of the FSPL formula and the need for direct line of sight and no inferences. Nevertheless, the SoC used in this work outperforms the ones used in literature in terms of sensitivity, throughput, and power consumption. For example, the one used by Maudet et al. [3], [17], [19] enables a PHY datarate of 5.8 Mbit s^{-1} with a sensitivity of −76 dBm. For a similar sensitivity, the SoC used in this work allows for a PHY datarate of 35 Mbit s^{-1}. When comparing the energy consumption, they calculate an EPB of hundreds of µJ. The work presented here outperforms it by orders of magnitude, with an EPB spanning from 27 nJ to 1312 nJ. Compared to the work presented by Lee et al. [4], the sensitivity is −81 dBm for a datarate of 13.5 Mbit s^{-1}. At such a sensitivity, the MM6108 can reach data rates of 26 Mbit s^{-1}.

C. Application Example

To compare the results of this test to a real-world scenario, this work is compared to BLE for the case of Aerosense [8]. Using a 17.5 dBi directional antenna, they manage to reach 275 m with a throughput of 938 kbit s^{-1} or 438 m with a data rate of 850 kbit s^{-1}. The EPB for communication varies between 80 nJ bit^{-1} and 180 nJ bit^{-1}. The closest result from our work is for an attenuation of 71 dB, which would correspond to a distance of 905 m when applying the process described in Section III-B for the same antenna gain. With a bandwidth of 8 MHz, this would lead to a throughput of 10.7 Mbit s^{-1}, outperforming the BLE approach by a factor of 10. The energy consumption is also lower, with 45 nJ bit^{-1}. Using Wi-Fi HaLow instead of BLE for this specific use case would enable continuous data streaming from multiple nodes while reducing the energy needed per bit. Furthermore, the gateway could be placed further away from the nodes and still maintain a high throughput, relying on other bandwidths if required. This shows the potential of HaLow for IoT devices and WSN.

D. Comparison to Other IoT Wireless Protocols

HaLow fits for applications requiring a high throughput and distances of a few kilometers to be covered, but other protocols (described in Table I) can outperform it in different

conditions. When the distance to cover is below 50 m and the throughput is not a bottleneck, like for wireless beacons, UWB or ZigBee have a lower energy consumption per bit. When a higher throughput is needed, for video streaming for instance, traditional Wi-Fi is more suitable. For longer distances, protocols like LTE, NB-IoT or LoRa are more suitable.

V. Conclusion

In this work, a reproducible evaluation framework for Wi-Fi HaLow is presented with distance mapping via FSPL, and application-level measurements of energy and throughput. The results confirm HaLow's ability to deliver multi-Mbps links as (from $0.15\,\mathrm{Mbit\,s^{-1}}$ to $18\,\mathrm{Mbit\,s^{-1}}$) over multi-kilometer ranges with an energy consumption going from $27\,\mathrm{nJ\,bit^{-1}}$ to $1312\,\mathrm{nJ\,bit^{-1}}$, and demonstrate its clear advantages when deployed compared to other IoT protocols. The use cases benefiting from HaLow are also detailed. Using off-the-shelf microcontroller-based hardware and a solid testing approach, this work gives a clear guide for future HaLow-based edge-IoT deployments. Future work will focus on the development of a custom HaLow node for WSN. Radiated tests will also be performed to confirm the capabilities of the technology.

References

[1] L. Tian, S. Santi, A. Seferagić, J. Lan, and J. Famaey, "Wi-Fi HaLow for the Internet of Things: An up-to-date survey on IEEE 802.11ah research," *Journal of Network and Computer Applications*, vol. 182, p. 103036, May 2021. [Online]. Available: https://www.sciencedirect.com/science/article/pii/S108480452100062X

[2] M. A. Jamshed, K. Ali, Q. H. Abbasi, M. A. Imran, and M. Ur-Rehman, "Challenges, Applications, and Future of Wireless Sensors in Internet of Things: A Review," *IEEE Sensors Journal*, vol. 22, no. 6, pp. 5482–5494, Mar. 2022. [Online]. Available: https://ieeexplore.ieee.org/document/9698203

[3] S. Maudet, G. Andrieux, R. Chevillon, and J.-F. Diouris, "Practical evaluation of Wi-Fi HaLow performance," *Internet of Things*, vol. 24, p. 100957, Dec. 2023. [Online]. Available: https://www.sciencedirect.com/science/article/pii/S2542660523002809

[4] I.-G. Lee, D. B. Kim, J. Choi, H. Park, S.-K. Lee, J. Cho, and H. Yu, "WiFi HaLow for Long-Range and Low-Power Internet of Things: System on Chip Development and Performance Evaluation," *IEEE Communications Magazine*, vol. 59, no. 7, pp. 101–107, Jul. 2021. [Online]. Available: https://ieeexplore.ieee.org/abstract/document/9502660

[5] S. Tschimben, K. Gifford, and R. Brown, "IEEE 802.11ah SDR Implementation and Range Evaluation," in *2019 IEEE Wireless Communications and Networking Conference (WCNC)*, Apr. 2019, pp. 1–6, iSSN: 1558-2612. [Online]. Available: https://ieeexplore.ieee.org/abstract/document/8885445

[6] T. Abderrahmane, A. Nourredine, and T. Mohammed, "Experimental analysis for comparison of wireless transmission technologies: Wi-Fi, Bluetooth, ZigBee and LoRa for mobile multi-robot in hostile sites," *International Journal of Electrical and Computer Engineering (IJECE)*, vol. 14, no. 3, pp. 2753–2761, Jun. 2024, number: 3. [Online]. Available: https://ijece.iaescore.com/index.php/IJECE/article/view/35322

[7] A. E. Basabi and S. M. Hashemi, "Energy Consumption Evaluation of ZigBee Routing Protocols in IOT," *Wireless Personal Communications*, vol. 130, no. 2, pp. 707–727, May 2023. [Online]. Available: https://doi.org/10.1007/s11277-022-10114-4

[8] T. Polonelli, H. Müller, W. Kong, R. Fischer, L. Benini, and M. Magno, "Aerosense: A Self-Sustainable and Long-Range Bluetooth Wireless Sensor Node for Aerodynamic and Aeroacoustic Monitoring on Wind Turbines," *IEEE Sensors Journal*, vol. 23, no. 1, pp. 715–723, Jan. 2023, conference Name: IEEE Sensors Journal. [Online]. Available: https://ieeexplore.ieee.org/abstract/document/9967940

[9] J. Imfeld, S. Cortesi, P. Mayer, and M. Magno, "Evaluation of a Non-Coherent Ultra-Wideband Transceiver for Micropower Sensor Nodes," in *2023 IEEE SENSORS*, Oct. 2023, pp. 1–4, iSSN: 2168-9229. [Online]. Available: https://ieeexplore.ieee.org/abstract/document/10325219

[10] V. Vomhoff, S. Raffeck, S. Gebert, S. Geissler, and T. Hossfeld, "NB-IoT vs. LTE-M: Measurement Study of the Energy Consumption of LPWAN Technologies," in *2023 IEEE International Conference on Communications Workshops (ICC Workshops)*, May 2023, pp. 403–408, iSSN: 2694-2941. [Online]. Available: https://ieeexplore.ieee.org/abstract/document/10283595

[11] M. Ballerini, T. Polonelli, D. Brunelli, M. Magno, and L. Benini, "Experimental Evaluation on NB-IoT and LoRaWAN for Industrial and IoT Applications," in *2019 IEEE 17th International Conference on Industrial Informatics (INDIN)*. Helsinki, Finland: IEEE, Jul. 2019, pp. 1729–1732. [Online]. Available: https://ieeexplore.ieee.org/document/8972066/

[12] C. Milarokostas, D. Tsolkas, N. Passas, and L. Merakos, "A Comprehensive Study on LPWANs With a Focus on the Potential of LoRa/LoRaWAN Systems," *IEEE Communications Surveys & Tutorials*, vol. 25, no. 1, pp. 825–867, 2023. [Online]. Available: https://ieeexplore.ieee.org/abstract/document/9990567

[13] T. Polonelli, "Ultra-low power IoT applications: from transducers to wireless protocols," Doctoral Thesis, Alma Mater Studiorum - Università di Bologna, Apr. 2021. [Online]. Available: https://amsdottorato.unibo.it/id/eprint/9604/

[14] T. Polonelli, D. Brunelli, A. Girolami, G. N. Demmi, and L. Benini, "A multi-protocol system for configurable data streaming on IoT healthcare devices," in *2019 IEEE 8th International Workshop on Advances in Sensors and Interfaces (IWASI)*. Otranto, Italy: IEEE, Jun. 2019, pp. 112–117. [Online]. Available: https://ieeexplore.ieee.org/document/8791381/

[15] N. Ahmed, D. De, F. A. Barbhuiya, and M. I. Hussain, "MAC Protocols for IEEE 802.11ah-Based Internet of Things: A Survey," *IEEE Internet of Things Journal*, vol. 9, no. 2, pp. 916–938, Jan. 2022. [Online]. Available: https://ieeexplore.ieee.org/abstract/document/9512279

[16] S. M. Soares and M. M. Carvalho, "Throughput Analytical Modeling of IEEE 802.11ah Wireless Networks," in *2019 16th IEEE Annual Consumer Communications & Networking Conference (CCNC)*, Jan. 2019, pp. 1–4, iSSN: 2331-9860. [Online]. Available: https://ieeexplore.ieee.org/abstract/document/8651805

[17] S. Maudet, G. Andrieux, R. Chevillon, and J.-F. Diouris, "Evaluation and Analysis of the Wi-Fi HaLow Energy Consumption," *IEEE Internet of Things Journal*, vol. 11, no. 17, pp. 28 244–28 252, Sep. 2024. [Online]. Available: https://ieeexplore.ieee.org/document/10531711/

[18] A. R. Ortigoso, G. Vieira, D. Fuentes, L. Frazão, N. Costa, and A. Pereira, "A Multi-Tenant SDN Architecture for Network Deployment Using a Wi-Fi HaLow-Based IEEE 802.11s Mesh," in *2024 IEEE Virtual Conference on Communications (VCC)*, Dec. 2024, pp. 1–6. [Online]. Available: https://ieeexplore.ieee.org/abstract/document/10914359

[19] S. Maudet, G. Andrieux, R. Chevillon, and J.-F. Diouris, "Refined energy consumption model of an STA in a Wi-Fi HaLow network," *IEEE Transactions on Communications*, pp. 1–1, 2025. [Online]. Available: https://ieeexplore.ieee.org/abstract/document/10857419

[20] S. Aust, "Measurement Study of IEEE 802.11ah Sub-1 GHz Wireless Channel Performance," in *2024 IEEE 21st Consumer Communications & Networking Conference (CCNC)*, Jan. 2024, pp. 847–850, iSSN: 2331-9860. [Online]. Available: https://ieeexplore.ieee.org/abstract/document/10454693

[21] K. K. Thangadorai, M. Prakash, M. Baddeley, A. Pandey, and K. M. Sivalingam, "Extending Boundaries with WiLong: A Field Study on Long-Range Wi-Fi Mesh Custom Solution," in *2024 IEEE 49th Conference on Local Computer Networks (LCN)*, Oct. 2024, pp. 1–9, iSSN: 2832-1421. [Online]. Available: https://ieeexplore.ieee.org/abstract/document/10639754

[22] B. Myagmardulam, N. Tadachika, K. Takahashi, R. Miura, F. Ono, T. Kagawa, L. Shan, and F. Kojima, "Path Loss Prediction Model Development in a Mountainous Forest Environment," *IEEE Open Journal of the Communications Society*, vol. 2, pp. 2494–2501, 2021. [Online]. Available: https://ieeexplore.ieee.org/abstract/document/9586048